Eur. Phys. J. D **45**, 179–187 (2007)
DOI: 10.1140/epjd/e2007-00250-2

THE EUROPEAN PHYSICAL JOURNAL D

# Photodetachment of $H^-$ in parallel electric and magnetic fields near an elastic surface

Dehua Wang[a]

College of Physics and Electronic Engineering, Ludong University, Yantai 264025, P.R. China

Received 6 May 2007 / Received in final form 22 June 2007
Published online 8 August 2007 – 

**Abstract.** Using the closed orbit theory, we give a clear physical picture description of the photodetachment of $H^-$ in parallel electric and magnetic fields near an elastic surface. It is found that the surface can produce some interesting effects. Besides the closed orbits previously found by Peters et al. for the $H^-$ in parallel electric and magnetic fields, some additional closed orbits are produced due to the effect of the elastic surface. The photodetachment cross section of this system is also derived and calculated. The results show that the cross section depends on the external field strength and the ion-surface distance, which is more complicated in contrast with the cross section of $H^-$ in parallel electric and magnetic fields without surface. Therefore we can control the photodetachment cross section of the negative ion by changing the external field strength and the ion-surface distance. This study provides a new understanding of the photodetachment process of negative ion in the presence of external field and surface.

**PACS.** 32.80.Gc Photodetachment of atomic negative ions – 03.65.Sq Semiclassical theories and applications – 34.50.Dy Interactions of atoms and molecules with surfaces

## 1 Introduction

It is well-known that the environment such as potential walls or cavities might have significant effect on the photodetachment cross section of ions and the photoabsorption spectra of atoms. Early experiment and theory showed that the photodetachment cross section of $H^-$ in the presence of external fields displays oscillatory structures [1–10]. In early 1979, Blumberg et al. studied the photodetachment of negative ions in a magnetic field, they found the cross section of negative ions in magnetic field was shown to have an oscillatory dependence on photon energy [6]. Later, Bryant et al. observed a ripplelike structure in the photodetachment cross section of $H^-$ in the presence of motional electric fields [1]. Rau and Wong explained this phenomenon using a frame-transformation theory [2]. Stewart analyzed the effects of electric fields on the photodetachment cross section of the $H^-$ ion near threshold [10]. In these early studies, they all considered the photodetachment of negative ion in a single electric or magnetic field. Subsequently, many theoretical studies of the photodetachment of $H^-$ in parallel or crossed electric and magnetic fields have been carried out by Fabrikant [7], Peters and Delos [3,4] and by other authors [8,9]. A generalization to the case of photodetachment of $H^-$ in the presence of static electric and magnetic field of arbitrary orientation has been given by Liu and Wang [5]. Among these studies, Du and Delos' closed orbit theory has provided a clear framework to understand the oscillation in the complicated spectra for atoms or negative ion in external fields [11]. They found that the oscillations were caused by the interference of the detached-electron waves reflected by the external fields and the outgoing detached-electron waves localized in the regions of the bound state of $H^-$.

Recently, much attention has been paid to the photo-induced electronic excitations of adsorbates on metal surfaces [12]. Since the $H^-$ has been proposed to use to probe adsorbate state lifetime and charge transfer during backscattering [13], the photodetachment of $H^-$ near an interface has attracted much interest. Firstly, Yang et al. used an elastic wall model for the electron scattering interface. They derived and calculated the photodetachment cross section of $H^-$ near an interface without and with a static electric field by using the closed orbit theory [14,15]. Then Afaq and Du discussed the photodetachment of $H^-$ near a reflecting interface using a theoretical imaging method [16]. In these early studies, they all considered the photodetachment of negative ion near a surface with or without electric field. To the best of our knowledge, no study of the photodetachment of ion near a surface in the presence of electric and magnetic fields has been reported. However, there is a need to do this study. With the development of photodetachment microscope technology, it is possible to observe the spatial distributions of detached-electron on a screen [17]. Theoretical

[a] e-mail: jnwdh@sohu.com

investigations on the detached electron distributions on a screen perpendicular to the parallel electric and magnetic fields show structures resulting from the interference of two distinctive electron paths [18,19]. Inspired by these early works, we study the photodetachment of $H^-$ in parallel electric and magnetic fields with an elastic surface perpendicular to the fields. For simplicity, we still consider the surface as an elastic reflecting wall, which can be seen as a dielectric film with the bottom of the conduction band well above the vacuum level. This assumption about the elastic wall is consistent with both experimental and theoretical studies of the microjunctions in the semiconductor device over the years [20–22]. Our study is based on the closed orbit theory. We obtain an analytical expression for the cross section as the sum of the contributions of the closed orbits. The cross section is related to the strength of the external fields and the distance between the ion and the surface, which suggest that we can control the photodetachment cross section by changing the external field strength and the ion-surface distance. The results show that due to the effect of the surface, the number of the closed orbits increased greatly and the oscillations in the photodetachment cross section become much more complicated than the case of the photodetachment of $H^-$ in parallel electric and magnetic fields without surface.

This paper is organized as follows: in Section 2, we study the classical motion of the detached electron of $H^-$ in parallel electric and magnetic fields near an elastic surface and find out the closed orbits of this system. In Section 3, we derive the photodetachment cross section of $H^-$ in parallel electric and magnetic fields near an elastic surface by using the closed orbit theory. In Section 4, we calculate the cross section for different distances between the ion and the surface and discuss the influence of the external fields on the photodetachment cross section. Section 5 gives some conclusions of this paper. Atomic units are used throughout this work unless indicated otherwise.

## 2 The classical motion

Take the directions of the electric and magnetic fields as the $z$-axis, a hydrogen negative ion $H^-$ sits at the origin and a $z$-polarized laser is applied for the photodetachment. An elastic surface perpendicular to $z$-axis is put at $z = -d$. So the photodetachment electron can be reflected by the external fields and the surface. The $H^-$ can be considered effectively as a one-electron system, with the active electron loosely bound by a short-range, spherically symmetric potential $V_b(r)$, where $r$ is the distance between the active electron and the origin where the nucleus is. In the cylindrical coordinates ($\rho$, $z$, $\phi$), the detached electron's Hamiltonian is (the electron spin is omitted):

$$H = \frac{1}{2}\left(P_\rho^2 + \frac{L_z^2}{\rho^2}\right) + \omega_L L_z + \frac{1}{2}\omega_L^2\rho^2 + \frac{1}{2}P_z^2 + Fz + V(z) + V_b(r). \quad (1)$$

In which $\omega_L = H/2c$ is the Larmor frequency, $F$ and $H$ are the electric and magnetic field strengths. $V(z)$ is the interaction between the electron and the elastic surface, it can be described as:

$$V(z) = \begin{cases} 0 & -d < z < +\infty \\ \infty & z \leqslant -d \end{cases}.$$

Due to the cylindrical symmetry of the system, the canonical angular momentum $L_z$ is a constant of motion. In our paper, the electron emerges from the center of the chosen coordinate system, so we take it as zero. Therefore, the Hamiltonian separates into the motion along the $z$-axis and the motion in the perpendicular $x - y$ plane. According to the closed orbit theory, we split the whole space into two spatial regions: (1) the core region inside a small sphere with the radius $R \approx 10a_0$ ($a_0$ is the Bohr radius), where the laser field and the core field influences exist, while the external fields can be neglected; (2) the outer region, where the influence of the external fields are more important and the interaction between the active electron and the residue of the ion can be neglected. In this area the electron only feels the presence of electric and magnetic fields. Therefore, we can use semiclassically closed orbit theory to describe the electron motion [11].

When the electron enters the outer region, the short-range potential $V_b(r)$ can be negligible. By solving the Hamiltonian motion equations, we get the classical motion equations of the detached electron [3]:

$$\begin{cases} \rho(t) = \frac{1}{\omega_L} k \sin\theta_{out} |\sin(\omega_L t)| \\ z(t) = k\cos\theta_{out} t - \frac{1}{2}Ft^2 \\ \phi(t) = \omega_L t + \phi_{out} \end{cases} \quad (2)$$

where $k = \sqrt{2E}$ is the momentum of the detached electron and $\theta_{out}$ is the emanating angle between the momentum and $z$-axis. From the motion equations, we find that the $z$-motion is uniform acceleration, and the motion in $\rho$ and $\phi$ is a cyclotron motion. The azimuthal motion in $\phi(t)$ can be neglected. Because the elastic surface is perpendicular to the $z$-direction, it has no influence on the $\rho$ motion. According to the closed orbit theory, every classical orbit of the detached electron that subsequently returns to the ion produces an oscillation in the photodetachment cross section. Considering the effect of the elastic surface, the closed orbits can be divided into three classes.

(i) This class of the closed orbits is the same as the ones of $H^-$ in parallel electric and magnetic fields without surface [3]. The electron was emitted from the origin with a certain initial momentum $k$ and initial angle $\theta_{out}$. For the $z$-motion, the time required to go from $z = 0$ up against the electric field force and then return to $z = 0$ is $t_{ret}^z = 2k\cos\theta_{out}/F$. The motion in $\rho$ is a sinusoidal oscillation and represents cyclotron motion in the magnetic field. The electron returns to $\rho = 0$ at each cyclotron period $t_{ret}^\rho = j\pi/\omega_L$, $j = 1, 2\ldots$ is the number of the cyclotron period. A closed orbit occurs whenever the electron goes out with energy and direction of motion such that $t_{ret}^z = t_{ret}^\rho$. These closed orbits are given in Figure 1a. In this part, we did not

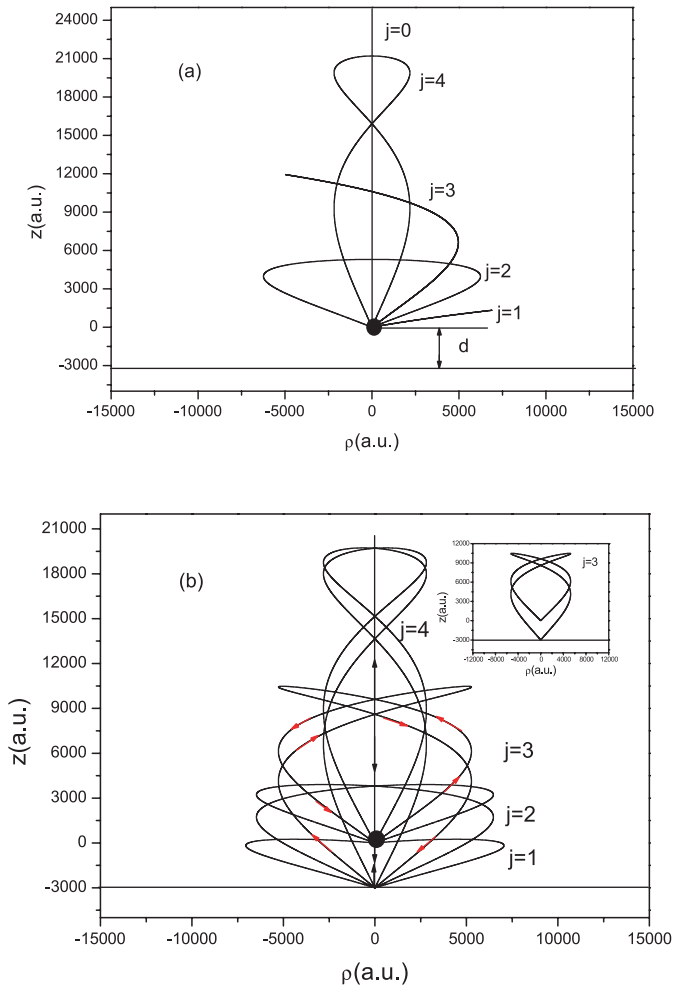


**Fig. 1.** (Color online) Schematic of the closed orbits of the detached electron of $H^-$ in parallel electric and magnetic fields near an elastic surface. The electric field and magnetic fields are along the $+z$-axis. $H^-$ is denoted by a black dot at the origin. The solid line at $d = 3000$ a.u. is the elastic surface. Figure (a) are the closed orbits as the ones given in [3]; figure (b) are the parallel and off-$z$-axis closed orbits due to the effect of the elastic surface, one closed orbit is indicated by red arrows for clarity. The inset plot is the $j = 3$ closed orbit.

consider the parallel orbit, which is given in the following part.

(ii) The parallel closed orbits along the $z$-axis. Similar to the photodetachment of $H^-$ in electric field near an elastic surface [15], there are four fundamental closed orbits along the $z$-axis. (a) The electron goes up along the $+z$-direction, reaches its maximum point, then pulls back by the electric field and returns to the origin. (b) The electron goes down in the $-z$-direction and hits the surface, then bounces back and finally returns to the origin. (c) The electron completes the first orbit and then passes through the origin, and continues to complete the second orbit. (d) This orbit is similar to the one of (c) but in reverse order, the electron completes the second orbit first and then the first orbit. This kind of closed orbits is given in Figure 1b as indicated by arrows.

The periods of these four fundamental closed orbits are:

$$T_1 = \frac{2k}{F}, \quad T_2 = \frac{-2k + 2\sqrt{k^2 + 2Fd}}{F},$$
$$T_3 = T_4 = T_1 + T_2 = \frac{2\sqrt{k^2 + 2Fd}}{F}. \tag{3}$$

The actions of these orbits are:

$$S_1 = \frac{4\sqrt{2}E^{3/2}}{3F}$$
$$S_2 = \frac{1}{12}F^2T_2^3 + \frac{1}{2}FkT_2^2 + k^2T_2$$
$$S_3 = S_4 = S_1 + S_2. \tag{4}$$

Maslov indices of these orbits can be found by counting the returning points [6], we have:

$$\mu_1 = \mu_2 = 1, \quad \mu_3 = \mu_4 = 2. \tag{5}$$

(iii) Off $z$-axis closed orbits. The electron emitted from the origin with a certain initial angle $\theta_j$, after traveling some time, it reaches the surface perpendicular to the $z$-axis at $z = -d$. This time $t_f$ can be calculated by using equation (2):

$$t_f = (k\cos\theta_j + \sqrt{k^2\cos^2\theta_j + 2Fd})/F. \tag{6}$$

The $\rho$ motion is the same as the cyclotron motion in the magnetic field. The cyclotron period is $T_c = \pi/\omega_L$. When $t_f = jT_c$ ($j = 1, 2...$), $\rho = 0$, the detached-electron reaches the $z$-axis and hits the surface. After bouncing back by the surface, the direction of the electron's velocity is changed. Hence after the collision of the electron with the surface, it will travel along the reverse direction as before it collides with the surface. After the same time $t_f$, it returns to the origin and forms a closed orbit. Some of the closed orbits are given in Figure 1b. In order to see this kind closed orbit clearly, we indicated one closed orbit by red arrows.

For each of these closed orbits, the period is

$$T_j = 2t_f = 2j\pi/\omega_L. \tag{7}$$

The initial angle is given by:

$$\cos\theta_j = -\frac{\omega_L d}{jk\pi} + \frac{jF\pi}{2k\omega_L}. \tag{8}$$

The action is:

$$S_j = \frac{1}{12}F^2T_j^3 - \frac{1}{2}FkT_j^2\cos\theta_j + k^2T_j\cos^2\theta_j + \frac{1}{2}k^2T_j\sin^2\theta_j. \tag{9}$$

Maslov indices of these orbits can be found by counting the number of the singular points such as focus and caustics they pass through [11].

## 3 The photodetachment cross section

The photodetached electron's wave function satisfies the Schrödinger equation with a source [23]:

$$[E - H(r,p)]\psi_d = D\psi_i \tag{10}$$

where $E$ is the energy of the detached electron, $D$ is the dipole operator: $D = a_x x + a_y y + a_z z$. For the linear polarized light along the $z$-axis, $a_x = a_y = 0$, $a_z = 1$. Then the dipole operator $D = Z$. $\psi_i$ is the initial wave function of $H^-$. In the present study we take the one electron approximation [24]. The initial wave function in configuration space is $\psi_i(r) = Be^{-k_b r}/r = R(r)/\sqrt{4\pi}$. Here $B = 0.31552$ is a normalization constant. $k_b = 0.2355883$, which is related to the binding energy $E_b$ of $H^-$ by $k_b = \sqrt{2E_b}$. When the dipole operator acts on the initial state, it produces a $p$ wave. For the linear $z$-polarized light,

$$|D\psi_i\rangle = rR(r)\chi(\theta). \tag{11}$$

Here $\chi(\theta) = \cos\theta/\sqrt{4\pi}$.

The physical solution of equation (10) requires only outgoing wave be present at large $r$. Once we have the wave function $\psi_d$ of the detached electron satisfying the correct outgoing boundary condition, the oscillator-strength density can be calculated by using the closed-orbit theory (COT). According to the COT, the photoabsorption cross section can be written as [11]

$$\sigma(E) = -\frac{4}{c}(E + E_b)\mathrm{Im}\langle D\psi_i|\hat{G}^+|D\psi_i\rangle \tag{12}$$

where $\hat{G}^+$ is the outgoing Green function. $|D\psi_i\rangle$ can be seen as a "source function". The Green function propagates these waves outward at fixed energy to become the outgoing waves. Due to the effect of the external fields and the elastic surface, these waves cannot propagate to infinity; some of the waves are turned back by the external fields or the surface and returned to the origin. The returning waves overlap with $|D\psi_i\rangle$ to give the interference pattern in the absorption spectrum.

According to closed orbit theory, the wave function $\psi_d$ can be separated into a direct part and a returning part:

$$\psi_d = \hat{G}^+_{dir}|D\psi_i\rangle + \hat{G}^+_{ret}|D\psi_i\rangle = (\psi_d)_{dir} + (\psi_d)_{ret}. \tag{13}$$

Accordingly, the cross section has two parts

$$\sigma(E) = \sigma_0(E) + \sigma^{ret}(E) \tag{14}$$

$\sigma_0(E)$ is the overlap integral of the direct part with the source function, it is the smooth background term in the cross section [15]:

$$\sigma_0(E) = \frac{16\sqrt{2}B^2\pi^2E^{3/2}}{3c(E_b + E)^3}. \tag{15}$$

The second part is the contribution of the returning wave:

$$\sigma^{ret}(E) = -\frac{4E_p}{c}\mathrm{Im}\langle D\psi_i|(\psi_d)_{ret}\rangle. \tag{16}$$

In which $(\psi_d)_{ret}$ represents the electron wave propagates outward into the external region first, then is pulled back by the external fields or reflected by the elastic surface and finally returns to the vicinity of the ion along all closed-orbits to interfere with the steady outgoing wave. It is a sum over returning wave associated with all the closed-orbit. At fairly large distances from the origin, the outgoing wave can be written as [3]:

$$\hat{G}^+_{dir}|D\psi_i\rangle \approx 2ikI_{l=1}(k)\chi(\theta)f^{(+)}_{out}(kr). \tag{17}$$

In which $I_l$ is the radial dipole integral and $f^{(+)}_{out}(kr) = e^{ikr}/kr$.

In order to obtain the returning wave function associated with each closed orbit, we draw a sphere of radius $R$, $R \approx 10a_0$. Outside this region, the atomic field strength is very small compared to the external fields and can be neglected. The outgoing wave on the surface of this sphere is then:

$$\psi^0(r) = (\hat{G}^+_{dir}|D\psi_i\rangle)_{r=R}. \tag{18}$$

When this wave propagates out from the surface and travels along the closed orbit, it changes phase and amplitude. In the semiclassical approximation, the wave outside this sphere is a sum of the above outgoing waves:

$$\psi(r) = \sum_i \psi^0(r)A_i e^{i[S_i - \mu_i\pi/2]} \tag{19}$$

where $S_i$ is the action along the $i$th trajectory, $\mu_i$ is the Maslov index characterizing the geometrical properties of the $i$th trajectory and $A_i$ is the amplitude [11].

If there are no external fields or elastic interface, the detached electron wave will propagate away from the source region near the nucleus as a spherical wave and never returns. But when there are external fields or elastic interface, the outgoing waves cannot propagate freely, some of the associated waves will turn back by the external fields or the surface. The returning wave function associated with each returning trajectory evaluated on the sphere with the radius $r_{ret}$ is given by

$$\psi^j_{ret}(r) = 2ikI_{l=1}(k)\chi(\theta^j_{out})f^{(+)}_{out}(kr_{out}) \times \left|\frac{J_j(t_0)}{J_j(t_{ret})}\right|^{1/2} e^{i[S_j(t_{ret}) - \mu_j\pi/2]} \tag{20}$$

where $J(t) = |\partial(x,y,z)/\partial(t,\theta,\varphi)| = \rho(t)\,|\partial(\rho,z)/\partial(t,\theta)|$ is the three-dimensional Jacobian at time $t$, which is related to the classical propagation amplitude $A_j$ by $A_j = |J_j(t_0)/J_j(t_{ret})|^{1/2}$ [11].

For the parallel electric and magnetic fields, due to the cylindrically symmetry, the returning wave near the origin can be approximated by a Bessel function:

$$f_{ret}(\rho,z) \approx \frac{1}{\sqrt{2\pi}}J_0(k^{ret}_\rho\rho)\frac{1}{\sqrt{2\pi}}e^{ik^{ret}_z z} \tag{21}$$

in which $J_0(k^{ret}_\rho\rho)$ is the zero-order Bessel function.

The incoming part of $f_{ret}(\rho, z)$ must match the semiclassical returning wave:

$$\psi^j_{ret}(r) \approx N_j f^{(-)j}_{ret}(\rho, z) \tag{22}$$

$N_j$ is a normalization factor:

$$N_j = 2ikI_{l=1}(k)\chi(\theta^j_{out})R_j e^{i[S_j(t_{ret})-\phi_j-\mu_j\pi/2]} \tag{23}$$

$R_j$ involves the ratio of Jacobians at $t = t_0$ and $t = t_{ret}$ and the outgoing and returning quantum waves [3]:

$$R_j = \left|\frac{f^{(+)j}_{out}}{f^{(-)j}_{ret}}\right| \left|\frac{J_j(t_0)}{J_j(t_{ret})}\right|^{1/2}. \tag{24}$$

Considering the influence of the surface, the closed orbits in this system include three classes, therefore this ratio must be considered separately.

For the first class of the closed orbits, $R_j$ is the same as the one given by Peters et al. except the parallel orbits. It is given by [3]:

$$R_j = 2\pi \left(\frac{\omega_L}{E}\right)^{1/2} j^{-1/2}. \tag{25}$$

Here $j$ =1, 2, 3... denotes the number of the closed orbit.

Next, we consider the parallel closed orbit along the $z$-axis. Since $\rho$ $(t)$ equals zero for all the time, the Bessel function in equation (21) should be equal to one, and the returning wave is approximated by a plane wave directed along the $z$-axis, $f^{(-)j}_{ret} = e^{\pm ikz}/2\pi$. The Jacobians at $t = t_0$ and $t = t_{ret} = T_j$ are given by:

$$J_j(t_0) = \sqrt{2E} r_0^2 \sin(\theta^j_{out}) \tag{26}$$

$$J_j(t_{ret}) = \frac{1}{\omega_L}\sqrt{2E}\sin(\theta^j_{out})\sin(\omega_L T_j)\frac{2E}{\omega_L} \times [1 + (-1)^j \frac{F}{\sqrt{2E}} T_j]\sin(\omega_L T_j). \tag{27}$$

Substituting the above equations into equation (24), $R_j$ is then given by

$$R_j = \frac{2\pi}{k}\frac{\omega_L}{\sin(\omega_L T_j)}\frac{1}{|[k^2 + (-1)^j F k T_j]|^{1/2}} \tag{28}$$

here, $j = 1, 2, 3, 4$ and $T_j$ is given by equation (3).

For the third kind closed orbits, $f^{(+)j}_{out}$, $f^{(-)j}_{ret}$ and $J_j(t_0)$ are the same as the first kind closed orbit [3], but with a different $J_j(t_{ret})$. The derivation of $J_j(t_{ret})$ is still valid as the first kind closed orbits but with a different period, which is $T_j = 2j\pi/\omega_L$. After a lengthy derivation, we find that $R_j$ is the same as given in equation (25).

The whole returning waves are the sum of each returning wave:

$$(\psi_d)_{ret} = \sum_j \psi^{ret}_j. \tag{29}$$

The overlap integral of the returning waves with the source wave function $\langle D\psi_i|$ gives the oscillation in the photodetachment cross section. Since the closed orbits are split into three classes, then $\sigma^{ret}(E)$ can be divided into three parts:

$$\sigma^{ret}(E) = \sigma^{ret}_1(E) + \sigma^{ret}_2(E) + \sigma^{ret}_3(E) \tag{30}$$

$\sigma^{ret}_1(E)$ corresponds to the contribution of the first kind of the closed orbits, which is the same as given in [3]:

$$\sigma^{ret}_1(E) = -6\sigma_0 \sum_{j=1}^{j_{max}} |R_j|\chi(\theta^j_{out})\chi^*(\theta^j_{ret}) \times \sin(S_j - \phi_j - \mu_j\pi/2). \tag{31}$$

Here $R_j$ is given by equation (25), $\phi_j = \pi/4$, $j_{max} = \text{int}[2k\omega_L/\pi F]$, $\mu_j$ is given in [3].

$\sigma^{ret}_2(E)$ corresponds to the contribution of the parallel closed orbits:

$$\sigma^{ret}_2(E) = (-1)^{\mu_j - 1}\frac{3}{2\pi}\sigma_0 \sum_{j=1}^{4} |R_j| \sin(S_j - \mu_j\pi/2). \tag{32}$$

In which $R_j$ is defined by equation (28), $S_j$ and $\mu_j$ are given by equations (4) and (5) separately.

$\sigma^{ret}_3(E)$ is the same as $\sigma^{ret}_1(E)$ but with different parameters. In this formula, $\theta^j_{out}$, $S_j$, $R_j$ are given by equations (8), (9) and (25), and $j_{max}$ is determined by equation (8), which is:

$$j_{max} = \text{int}\left[\frac{\omega_L(k + \sqrt{k^2 + 2Fd})}{\pi F}\right]. \tag{33}$$

Therefore, the total photodetachment cross section is

$$\sigma(E) = \sigma_0(E) + \sigma^{ret}_1(E) + \sigma^{ret}_2(E) + \sigma^{ret}_3(E) \tag{34}$$

which is a smooth background term plus many sinusoidal oscillatory terms.

## 4 Results and discussions

Using equation (34), we calculated the photodetachment cross section of $H^-$ in parallel electric and magnetic fields near an elastic surface for different values of the distance between the ion and the surface and different external field strength, see Figures 2–4.

In our calculation, the detached electron's energy is varied between 0 and 0.4 eV and we only consider the contribution of the primitive closed orbits to the cross section, the repetitions of the closed orbits are neglected. In Figure 2, we keep the electric field $F = 100$ V/cm, the magnetic field $B = 2.0$ T, then we change the distance between the ion and the surface. From this figure, we can see how the pattern of the photodetachment cross section changes with the increasing distance between the ion and the elastic surface. Figure 2a is the photodetachment cross section of $H^-$ in parallel electric and magnetic fields without surface, which is plotted for comparison [3]. Actually, when the distance is very large, $d \to +\infty$, the third class

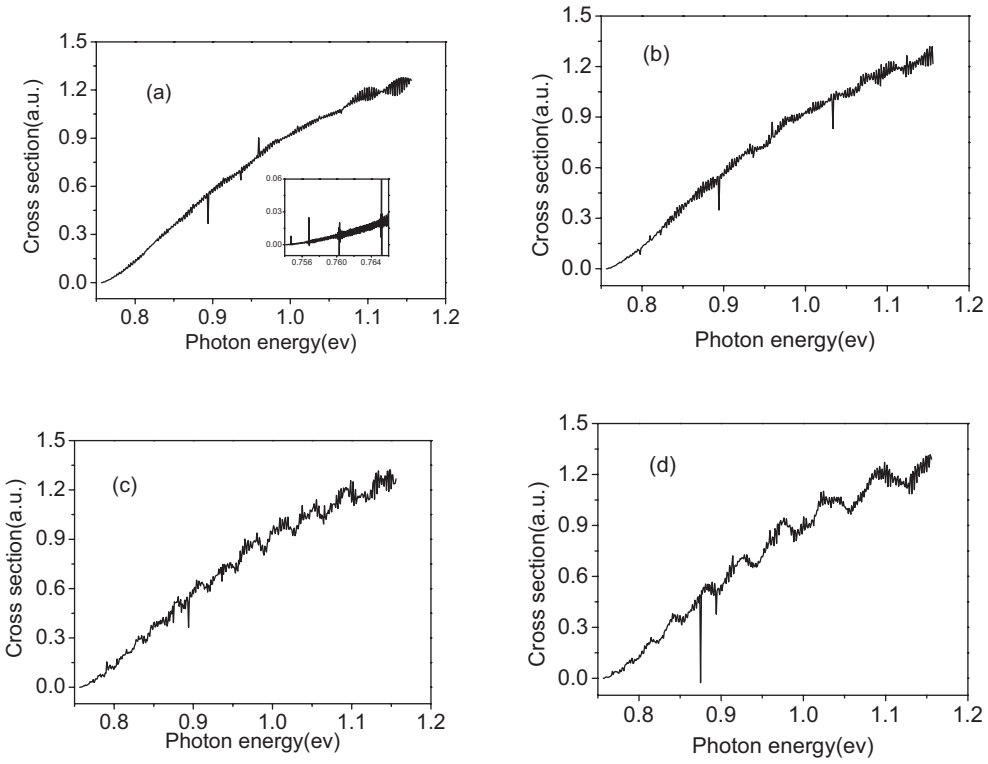


**Fig. 2.** The photodetachment cross section of $H^-$ in parallel electric and magnetic fields near an elastic surface. The electric field $F = 100$ V/cm and the magnetic field $H = 2.0$ T. The distances between the $H^-$ and the surface are: (a) $d \to +\infty$, this case equals to the photodetachment cross section of $H^-$ in parallel electric and magnetic fields without elastic surface, the inset plot is the cross section near the detachment threshold [3]. (b) $d = 7000$ a.u.; (c) $d = 300$ a.u.; (d) $d = 200$ a.u.

of the closed orbit and some of the parallel orbit no longer exist, therefore the present system should recover to the case of the photodetachment of $H^-$ in parallel electric and magnetic fields. When $d = 7000$ a.u., the cross section is shown in Figure 2b. We found that the spectrum changed a little from the one without surface. As we put the surface closer to the ion, the influence of the surface becomes significant. Figure 2c plots the cross section when the surface is 300 a.u. from the ion, we can see the cross section changes greatly from Figure 2a. If the surface approaches the ion further, the oscillations in the cross section become much more complicated, see Figure 2d. The reasons are as follows: the closer the surface moves to the ion, the more the returning waves bounced back by this surface, therefore, their contribution to the cross section becomes greater. In Figure 2, some irregular peaks appear. For example, in Figure 2a, there are sharp peaks at 0.9 eV and 0.97 eV. They are caused by the bifurcation of the closed orbits [3]. In fact, semiclassical theory predicts that the recurrence amplitude diverges at every bifurcation. Because a bifurcation is correlated with a focus of classical orbits, which lead to vanishing denominators in the cross section of $\sigma_2^{ret}(E)$. As to this problem, we will modify it by using the uniform semiclassical approximation in the following paper [25].

Next, we show how the electric and magnetic field influences the photodetachment cross section for fixed distance between the ion and the surface. We choose $d = 200$ a.u. as the ion-surface distance, since this distance is 10.6 nm and is quite typical in surface physics and cavity quantum dynamics. If both the electric and magnetic fields are present, the pattern of the spectrum changes as the relative strength of the two fields varies. The relative strength of the two fields is defined as: $R = F^{2/3}/2\omega_L$. If $R < 1$, the magnetic field dominates, the spectrum is characterized by the broad Landau envelope. But if $R > 1$, the electric field dominates and the spectrum is similar to the pattern in the presence of only the electric field [10]. Firstly, we keep $F = 100$ V/cm, then we change the magnetic field from 4.7 T to $10^{-6}$ T, see Figure 3. Figure 3a is the cross section when $H = 4.7$ T, under this condition, $R = 0.362$ is small than 1. The lorentz force acting on the detached electron is very strong. As the electron moves in the external fields, the cyclotron period in the $\rho$ motion $t_{ret}^{\rho} = j\pi/\omega_L$ is small. Then after a short period of time, the electron is turned back by the magnetic field and the elastic surface to the origin. Under this condition, the number of the closed orbit is great and the oscillation in the cross section is much more complicated. The broad Landau level envelope dominates the whole pattern of the spectrum. With the decrease of the magnetic field, the relative strength of the two fields $R > 1$, the electric field force dominates. The lorentz force is weak and the number of the closed orbit decreased. Thus the oscillation in the cross section becomes weaker, as we can see from Figures 3b and 3c. The whole pattern of the cross section looks like the one in the presence of only the electric field, the Landau resonances are nearly washed out by the electric field [15]. When the magnetic field is very small, for example $H = 10^{-6}$ T, in atomic unit, this number is very small and can be considered as zero. Then the influence of the magnetic field can be neglected. The present system recovers to the photodetachment of $H^-$ in electric field near an elastic surface. Only the closed orbits along

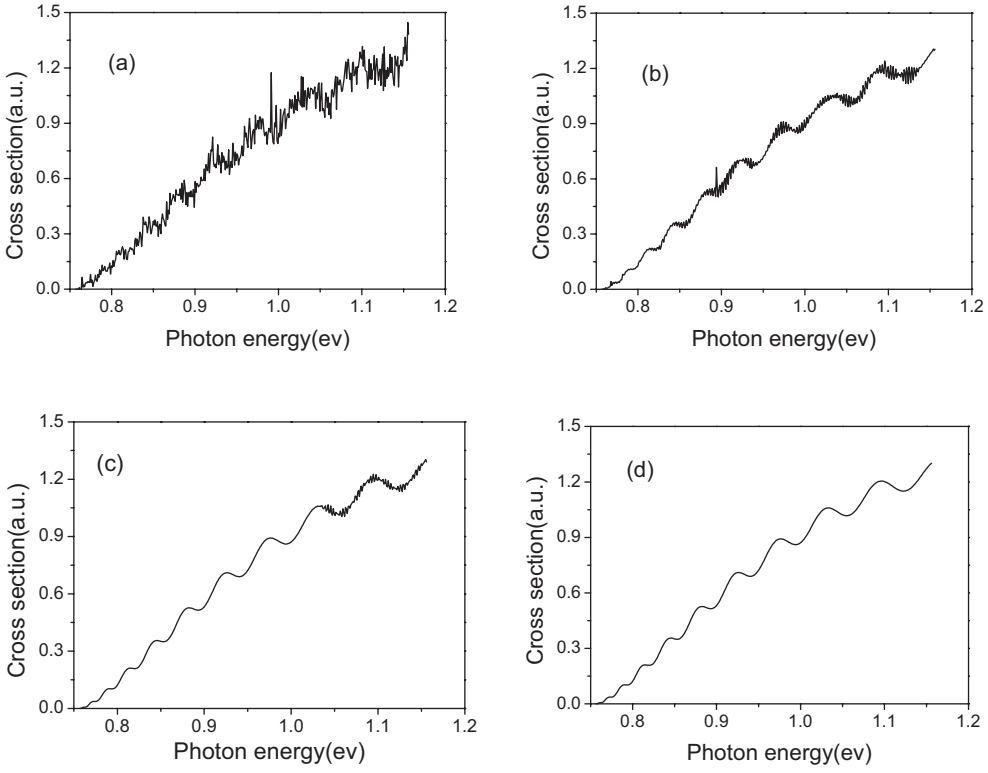


**Fig. 3.** The dependence of the photodetachment cross section on the magnetic field. The electric field $F = 100$ V/cm and the surface is fixed at $d = 200$ a.u. The magnetic fields are: (a) $H = 4.7$ T; (b) $H = 1.0$ T; (c) $H = 0.1$ T; (d) $H \to 0$.

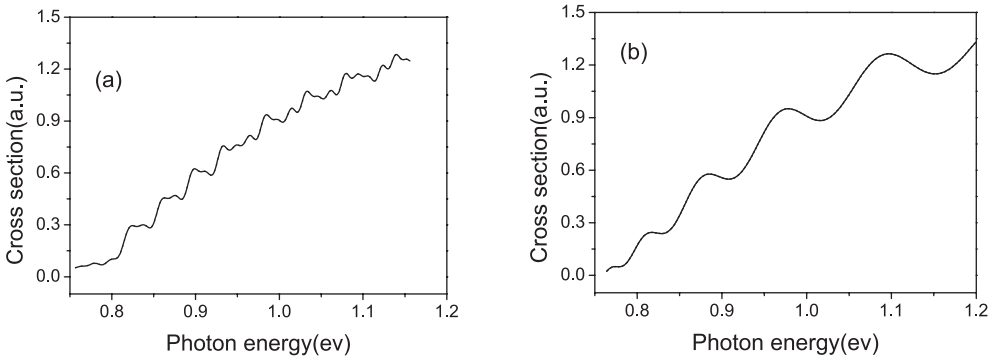


**Fig. 4.** The dependence of the photodetachment cross section on the electric field as $H \to 0$. (a) $F = 200$ KV/cm, $d = 300$ a.u., the solid line is our result and the dashed line is the one given in [15], which equals to the photodetachment cross section of $H^-$ in electric field near an elastic interface. (b) The photodetachment cross section with $F = 1$ V/cm, $d = 100$ a.u. The solid line is our calculation result and the dashed line is the result by using the imaging method [16].

the $z$-axis exist. Since $F = 100$ V/cm, this number is still small in atomic unit, its influence on the cross section is very small. The oscillations in the cross section is similar to the photodetachment of $H^-$ near an elastic surface without electric field [14], see Figure 3d.

In order to compare our result with the one given before, we consider two limit cases. First, we choose $F = 200$ kV/cm, the ion-surface distance $d = 300$ a.u., then we let $H \to 0$. The calculation result is shown in Figure 4a. The solid line in this plot is our result and the dashed line is the result given by Yang et al. [15], they are nearly the same. In fact, when $H \to 0$, the $R_j$ in equation (25) becomes zero, then $\sigma_1^{ret}(E)$ and $\sigma_3^{ret}(E)$ in the cross section vanished. $R_j$ in equation (28) becomes:

$$R_j = \frac{2\pi}{k} \frac{1}{T_j |[k^2 + (-1)^j F k T_j]|^{1/2}}. \tag{35}$$

And the total photodetachment cross section becomes:

$$\sigma(E) = \sigma_0(E) + (-1)^{\mu_j - 1} \frac{3}{k} \sigma_0 \times \sum_{j=1}^{4} \frac{1}{T_j |[k^2 + (-1)^j F k T_j]|^{1/2}} \sin(S_j - \mu_j \pi/2). \tag{36}$$

This is the photodetachment cross section of the $H^-$ in electric field near an elastic interface [15], only the parallel

**Table 1.** The period (in unit of $T_c$) and boundary energy $E_b$ (in unit of $\mathrm{cm}^{-1}$) of the first and third kind closed orbit with the electric field $F = 100$ V/cm, the magnetic field $H = 2.0$ T, and the distance between the ion and the surface $d = 200$ a.u. The first kind orbit is denoted by I in the superscript while the third kind orbit denoted by III.

| $j$ | 1 | 2 | 3 | 4 | 5 | 6 | 7 | 8 | 9 |
|---|---|---|---|---|---|---|---|---|---|
| $E_{bj}^{I}$ | 5.65 | 22.64 | 50.93 | 90.55 | 141.49 | 203.75 | 277.33 | 362.22 | 458.44 |
| $T_j^I$ | 1 | 2 | 3 | 4 | 5 | 6 | 7 | 8 | 9 |
| $E_{bj}^{III}$ | 5.24 | 22.21 | 50.51 | 90.13 | 141.06 | 203.32 | 276.90 | 361.80 | 458.01 |
| $T_j^{III}$ | 2 | 4 | 6 | 8 | 10 | 12 | 14 | 16 | 18 |

closed orbits contribute to the cross section under this condition. In Figure 4b we calculate the cross section with $F = 100$ V/cm, $d = 100$ a.u., $H \to 0$ by using our formula and the one given by Afraq and Du [16], they are correspondence with each other, which suggest our calculation is correct.

Finally, we discuss the variation of the electron's maximum kinetic energy $E_f^{max}$ with the number of the closed orbits. The energy at which a new closed orbit appears is called the boundary energy $E_b$ [3]. For the first kind closed orbit, the boundary energy is given by $E_{bj}^{I} = \frac{1}{2}(\frac{jF\pi}{2\omega_l})^2$; while for the third kind closed orbit, $E_{bj}^{III} = \frac{1}{2}(\frac{jF\pi}{2\omega_l} - \frac{d\omega_l}{j\pi})^2$. In Table 1, we give some of the period, the boundary energy $E_b$ of the first and third kind closed orbit with the electric field $F = 100$ V/cm, the magnetic field $H = 2.0$ T, and the distance from the ion to the surface $d = 200$ a.u. In Figure 5, we plot the variation of the electron's maximum kinetic energy with the number of the closed orbits. From this figure, we find as the electron's energy is very small, there are only 4 closed orbits, which are the ones along the $z$-axis. As the energy increased to 5.24 $\mathrm{cm}^{-1}$, the first off $z$-axis orbit appears, which belongs to the third kind closed orbit. There are altogether 5 closed orbits. As $E_f^{max}$ increased to 5.65 $\mathrm{cm}^{-1}$, another off $z$-axis orbit appears, which belongs to the first kind closed orbit. There are altogether 6 closed orbits. With the increase of $E_f^{max}$, the number of the closed increased greatly. As $E_f^{max}$ increased to 460 $\mathrm{cm}^{-1}$, there are 22 closed orbits. The more the closed orbits, the more complicated oscillation in the cross section. As we can see from Figures 2–4.

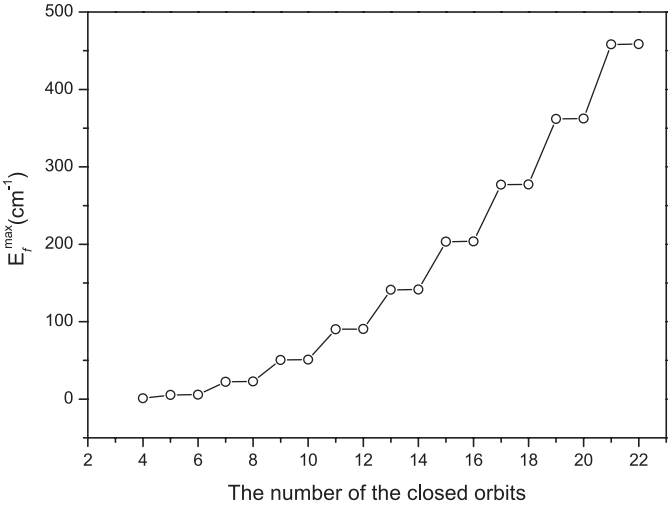


**Fig. 5.** The variation of the electron's maximum kinetic energy with the number of the closed orbits.

## 5 Conclusion

In summary, we have studied the photodetachment of $H^-$ in parallel electric and magnetic field near an elastic surface by using the closed orbit theory. We find that the elastic surface has significant influence on the photodetachment process, it produces some interesting phenomenon. Considering the influence of the elastic surface, the number of the closed orbits is increased greatly and the oscillations in the photodetachment cross section become much more complicated in contrast with none surface exists. This study provides a general framework for the understanding of the photodetachment process of $H^-$ in the presence of external field and surface. In this paper, we consider the surface as an elastic wall, this is only a simple model. As to the metal interface, the method we used in this paper cannot be directly applied to these real systems, but a generalization of our semiclassical method to a more elaborate system is straightforward once an accurate potential between the ion and metal surface is available. The theoretical calculation and analysis of the photodetachment of ion near a metal surface is in progress. In the next work, we will carry out the quantum calculation and compare our semiclassical closed orbit theory result with the quantum result. At present, no experiments on this system are available for comparison. We hope that our results will be useful in guiding the future experimental research of the photodetachment processes of ions in the vicinity of interfaces, cavities and ion traps [26].

This research has been supported by the National Natural Science Foundation of China (Grant No. 10604045 & 10674114) and the Doctoral Scientific Research Startup Foundation of Ludong University (Grant No. 202-23000301). I also thank the referees for some useful suggestions.

## References

1. H.C. Bryant et al., Phys. Rev. Lett. **58**, 2412 (1987)
2. A.R.P. Rau, H. Wong, Phys. Rev. A **37**, 632 (1988)
3. A.D. Peters, C. Jaffe, J.B. Delos, Phys. Rev. A **56**, 331 (1997)

4. A.D. Peters, J.B. Delos, Phys. Rev. A **47**, 3020 (1993); A.D. Peters, J.B. Delos, Phys. Rev. A **47**, 3036 (1993)
5. Z.Y. Liu, D.H. Wang, Phys. Rev. A **55**, 4605 (1997); Z.Y. Liu, D.H. Wang, Phys. Rev. A **56**, 2670 (1997)
6. W.A.M. Blumberg, W.M. Itano, D.J. Larson, Phys. Rev. A **19**, 139 (1979)
7. I.I. Fabrikant, Phys. Rev. A **43**, 258 (1991)
8. J.N. Yukich, T. Kramer, C. Bracher, Phys. Rev. A **68**, 033412 (2003)
9. Q. Wang, A.F. Strarace, Phys. Rev. A **51**, 1260 (1995)
10. M.L. Du, Phys. Rev. A **40**, 1330 (1989)
11. M.L. Du, J.B. Delos, Phys. Rev. A **38**, 1896 (1988)
12. H. Petek, M.J. Weida, H. Nagano, S. Ogawa, Science **288**, 239 (1999)
13. J. Sjakste, A.G. Borisov, J.P. Gauyacq, Phys. Rev. Lett. **92**, 1561015 (2004)
14. G.C. Yang, Y.Z. Zheng, X.X. Chi, J. Phys. B **39**, 1855 (2006)
15. G.C. Yang, Y.Z. Zheng, X.X. Chi, Phys. Rev. A **73**, 043413 (2006)
16. A. Afaq, M.L. Du, J. Phys. B **40**, 1309 (2007)
17. C. Blondel, C. Delsart, F. Dulieu, Phys. Rev. Lett. **77**, 3755 (1996)
18. C. Bracher, J.B. Delos, Phys. Rev. Lett. **96**, 100404 (2006)
19. S. Gao, G.C. Yang, S.L. lin, M.L. Du, Eur. Phys. J. D **42**, 189 (2007)
20. C.M. Marcus et al., Phys. Rev. Lett. **69**, 506 (1992)
21. C.D. Schwieters, J.A. Alford, J.B. Delos, Phys. Rev. B **54**, 10652 (1996)
22. A. Haran et al., Eur. Phys. J. B **8**, 445 (1999)
23. N.D. Gibson, B.J. Davis, D.J. Larson, Phys. Rev. A **48**, 310 (1993)
24. M.L. Du, J.B. Delos, Phys. Rev. A **38**, 5609 (1988)
25. A.D. Peters, C. Jaffe, J. Gao, J.B. Delos, Phys. Rev. A **56**, 345 (1997)
26. G.R. Lloyd, S.R. Procter, T. Softley, Phys. Rev. Lett. **95**, 133202 (2005)